THE ASTROPHYSICAL JOURNAL, 396:L75–L78, 1992 September 10

OUTFLOWING MOLECULAR GAS IN NGC 3079

JUDITH A. IRWIN
Department of Physics, Queen's University, Kingston, Ontario, Canada K7L 3N6
AND
YOSHIAKI SOFUE
Institute of Astronomy, The University of Tokyo, Mitaka, Tokyo 181, Japan
Received 1992 May 6; accepted 1992 June 29

ABSTRACT

High-resolution ^{12}CO ($J = 1$–0) observations of the radio lobe spiral galaxy NGC 3079 using the Nobeyama Millimeter-Wave Array show a dense, rigidly rotating ring of molecular gas with a radius of 750 pc. In addition, there is a molecular component which is tilted by 40° from the major axis and is aligned with the direction of the VLBI jet. This tilted component shows no appreciable rotation or expansion/contraction and is interpreted as molecular gas which is being accelerated out of the plane by the nuclear jet. Additional CO spurs and radio continuum ridges perpendicular to this feature are also present, suggesting that several outflow directions might be present.

Subject headings: galaxies: individual (NGC 3079) — galaxies: jets — ISM: molecules

1. INTRODUCTION

The edge-on spiral galaxy NGC 3079 is noteworthy for unusual kiloparsec-scale radio lobes emerging from its nucleus perpendicular to the plane (Hummel, van Gorkom, & Kotanyi 1983). The evidence, to date, suggests that the nuclear activity originates from an active galactic nucleus (AGN) rather than a starburst (Irwin & Seaquist 1988) and may be fueled by an inner molecular disk (Young, Claussen, & Scoville 1988). Line widths of CO (Young et al. 1988) and OH (Haschick & Baan 1985) are far in excess of normal galactic rotational velocities and are undoubtedly associated with gas in the nuclear vicinity. Indeed, at a distance of 15.6 Mpc ($H_0 = 75$ km s^{-1} Mpc^{-1}), NGC 3079 may be the closest "double-lobed radio source" to us, allowing the interaction between the nuclear outflow and the affected interstellar medium to be probed ($1'' = 75$ pc). The galaxy has been studied previously in some detail (Duric, Seaquist, & Davis 1983; Ford et al. 1986; Duric & Seaquist 1986; Irwin & Seaquist 1990, 1991; Filippenko & Sargent 1992). In this paper, we present high-resolution ($4'' \approx 300$ pc) CO observations using the Nobeyama five-element Millimeter-Wave Array (NMA) and report the discovery of an inner tilted component of molecular gas. A thorough description of the observations and results will be given in a separate paper (Sofue & Irwin 1992).

2. NMA OBSERVATIONS

^{12}CO ($J = 1$–0) line observations of NGC 3079 were made using the NMA in the C and D (compact) configurations, resulting in a synthesized HPBW of $4''.07 \times 3''.55$ (305 pc × 266 pc). C-array observations were made on 1991 January 28–29 and February 4–5, and D-array observations on 1991 January 4–5 and 13–14. The center position of the galaxy was taken to be at R.A. = $09^h58^m35^s.02$ and decl. = 55°55′15″.4 (1950), which corresponds to the radio continuum peak (Irwin & Seaquist 1991). The total bandwidth was 320 MHz (831 km s^{-1}), and data were averaged over 16 original frequency channels, resulting in a final frequency (velocity) resolution of 5 MHz (13 km s^{-1}). After Fourier-transforming to the sky plane, the resulting 64 channels were then CLEANed. No continuum emission was detected to a limit of 23 mJy beam^{-1}, as measured over the average of all line-free channels on either end of the band.

3. THE NUCLEAR MOLECULAR DISK

Figure 1 shows the integrated intensity map of NGC 3079 in the CO line. The nuclear molecular disk is clearly visible elongated at a position angle of −15°, which is the direction of the major axis of the optical and radio continuum disk. These results confirm previous ^{12}CO ($J = 1$–0) observations from the Owens Valley Millimeter-Wave Array (resolution: $8''.3 \times 6''.1$), which inferred the existence of a dense molecular disk within the central 14″ (Young et al. 1988). The brightness temperatures within our smaller NMA beam are somewhat higher than the Owens Valley measurements (cf. our maximum of $T_B = 8.2$ K compared with their ≈ 3 K over an equivalent 52 km s^{-1} velocity resolution), resulting in a total H_2 mass of $10.6 \times 10^9 (D/15.6\ \mathrm{Mpc})^2\ M_\odot$ in the nuclear disk [using $N(\mathrm{H_2})/\int T_B\,dV = 4 \times 10^{20}$ cm^{-2} (K km s^{-1})$^{-1}$; Young & Scoville 1982]. This is a factor of 4 higher than the previous value of $5.7 \times 10^9 (D/24\ \mathrm{Mpc})^2\ M_\odot$ (Young et al. 1988) and is a lower limit to the total H_2 mass, since the NMA did not detect all of the CO emission (see the "negative bowl" contours in Fig. 1). The total dynamical mass of the nuclear molecular disk is estimated from the rotation velocity to be $\sim 1.8 \times 10^{10} (D/15.6)\ M_\odot$, or about 1.7 times the H_2 mass in the same region. Therefore, the molecular gas makes up 50%–60% of the total dynamical mass of the nuclear disk. This $M_{\mathrm{H_2}}/M_{\mathrm{dyn}}$ ratio is large compared with normal galactic disks, but appears to be typical for the central regions of CO or IR-bright galaxies (e.g., Sofue 1988; Young & Scoville 1991).

In the inner, rigidly rotating part of the nuclear disk (i.e., $r < 5''.4$, or 400 pc), the H_2 mass is estimated to be $\sim 5.4 \times 10^9 (D/15.6\ \mathrm{Mpc})^2\ M_\odot$. If this mass is uniformly distributed within an edge-on ellipsoid, then the average molecular hydrogen density in this region is $n_{\mathrm{H_2}} = 530 (D/15.6\ \mathrm{Mpc})^{-1}$ cm^{-3}, and the rotational kinetic energy is $E = \frac{1}{2} I\omega^2 \sim 3 \times 10^{57} (D/15.6\ \mathrm{Mpc})^2$ ergs. For comparison, the Galactic center values are $n_{\mathrm{H_2}} = 60$–120 cm^{-3} within an equivalent region (Scoville & Sanders 1987) and $E = 10^{53}$ ergs within 300 pc (Bania 1977).

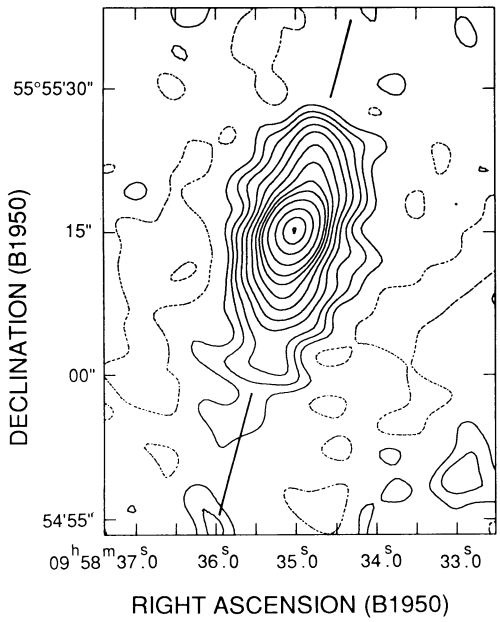

FIG. 1.—Total intensity ^{12}CO ($J = 1$–0) map of NGC 3079, where the intensity scale is the brightness temperature averaged over 700 km s^{-1} around the center frequency. The peak brightness temperature toward the nucleus is 5.13 K T_B, and contours are at 0.3 K $T_B \times -0.5$ (*dashed lines*), 0.5, 1, 1.5, 2.25, 3, 4, 5, 6, 7, 9, 12, 15, and 17. The solid line at P.A. = −15° denotes the major axis.

Figure 2*a* (Plate L7) shows the distribution of intensity-weighted mean velocities (e.g., van Gorkom & Ekers 1986), where the major axis is taken to be vertical. The velocity field clearly indicates galactic rotation about the minor axis, with a systemic LSR velocity of 1150 ± 10 km s^{-1}. Approximately equal amounts of redshifted and blueshifted gas are present overall, in contrast to the asymmetric ^{12}CO ($J = 1$–0) velocity profile from the IRAM 30 m telescope (J. Braine, private communication), which shows excess redshifted emission; the latter has likely been resolved out of the NMA data. Rigid rotation occurs within ≈5.″4 (400 pc), at which V_{max} = 330 km s^{-1}, with flatter rotation in the outer disk. Isovelocity contours near the systemic velocity show sharp bends toward the northeast and southwest, due to a contribution from the tilted component (see § 4 below). Beyond a radius of ∼10″ (750 pc), the nodal line of the disk is inclined by about +10° from the assumed major axis, i.e., at an unrotated position angle of −5°. This curvature of the CO major axis is also visible in the contours of the total intensity map (Fig. 1) (whether or not the tilted component is included in the sum) and, in addition, is seen in 20 cm radio continuum contours at the same spatial resolution (see Fig. 2 of Duric et al. 1983). Such behavior is typical of warped disks, but in this case it could also indicate the beginning of trailing molecular gas as the rotation curve turns over between 5.″4 and 10″ (note that the galaxy rotates "clockwise").

4. THE TILTED COMPONENT

Figure 3 shows the CO emission integrated over 104 km s^{-1} in velocity, centered at V_{LSR} = 1164 km s^{-1}. Most conspicuous in this figure is a *tilted component* which is inclined about 40° from the major axis (i.e., P.A. = −55°). At larger radii, especially noticeable on the northwest side, the contours curve in a "trailing" sense. Spurs perpendicular to this tilted component are also visible, with the whole structure resembling an inclined "cross."

Although not obvious in the total intensity CO image (Fig. 1), the tilted component is highly visible in Figure 2*b* as an inclined region of high velocity dispersion (reverse integral sign shape) within the nuclear molecular disk. At projected radii ≳3″ or 4″ northwest/southeast, the high velocity dispersion is due to the presence of the tilted component as a *distinct* velocity feature, as illustrated in the upper inset. When both velocity components are fitted with Gaussians and integrated over velocity separately, the velocity component closest to V_{sys} is clearly seen to be associated with the tilted component. On the northwest side, this velocity component is identifiable at radii down to $r \approx 2''$ (Fig. 2*b*, *lower inset*). It is lost at the galaxy center, where single, very broad lines are observed (central dark region of Fig. 2*b*), although one *might* interpret the existence of a narrow, apparent absorption dip at V_{sys} (see Fig. 1*b* of Sofue & Irwin 1992) as indicating the presence of two components here as well.

By Gaussian fitting, we find that the average FWHM of the tilted component is ≈30 km s^{-1} and the mass of the tilted component at $r > 4''$ on the northwest side alone is $\approx 10^8 (D/15.6)^2\ M_\odot$, which will be a lower limit to the total mass of the feature. Although the velocity (with respect to V_{sys}) of the *main disk* increases rapidly to ±178 km s^{-1} at the outermost measurable positions northwest and southeast, the velocity of the *tilted component* remains within ±30 km s^{-1} of V_{sys} at *all* radii, displaying only a small velocity gradient in the same sense as galactic rotation. The observed velocities are an order of magnitude smaller than those expected if the dynamics are governed by the interior ($10^{10}\ M_\odot$) gravitational potential. With

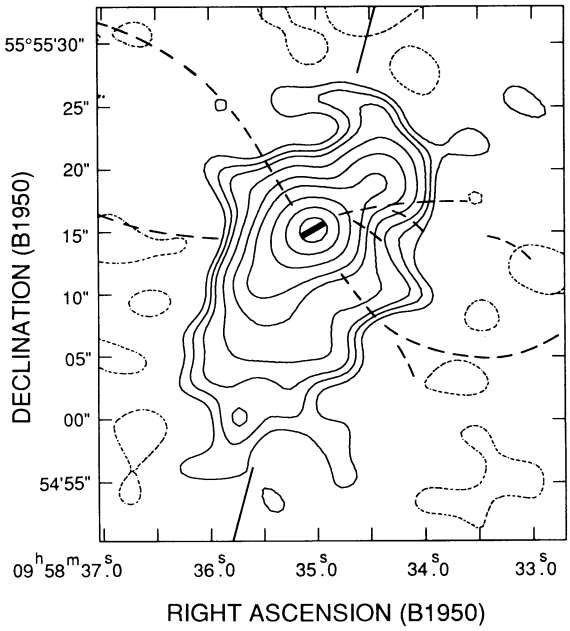

FIG. 3.—Average emission over a velocity range of 104 km s^{-1} centered at 1164 km s^{-1}, showing the tilted component at P.A. = −55° and the perpendicular spurs. Contours are at −0.05 (*dashed lines*), 0.5, 0.075, 0.10, 0.15, 0.22, 0.31, 0.50, 0.75, and 1.00 Jy beam^{-1} (× 6.4 to convert to K T_B). The solid black line denotes the major axis, and the heavy black bar in the center shows the VLBI angle (size exaggerated). The heavy dashed curves show the radio continuum ridges and boundaries of the radio lobes as traced from Fig. 1*a* of Duric & Seaquist (1986).

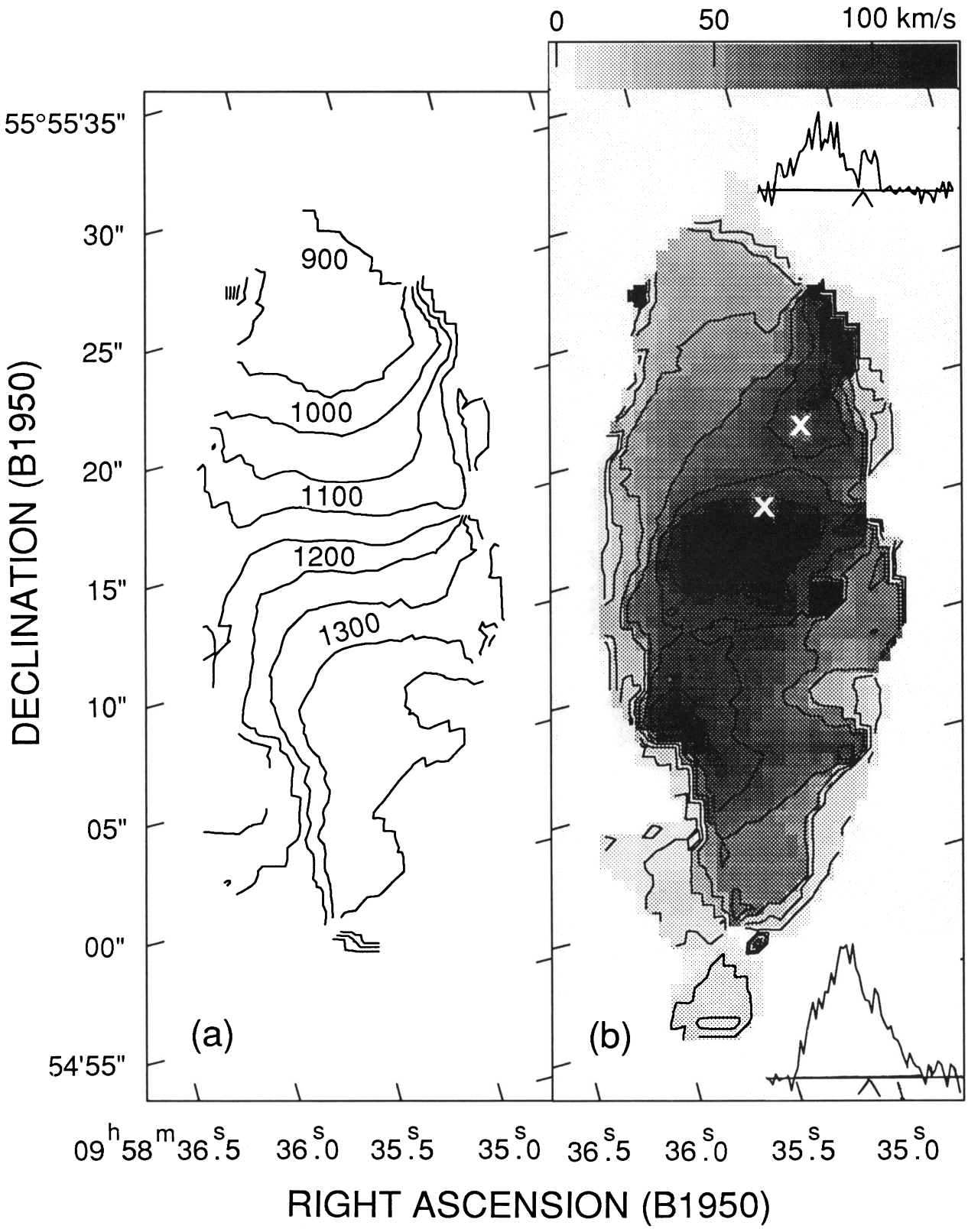

FIG. 2.—(*a*) Mean velocity field of NGC 3079, with the major axis vertical. Contours are separated by 50 km s^{-1}, with LSR velocities indicated on every other contour. (*b*) Velocity dispersion. Contours are 10, 25, 50, 75, 95, and 110 km s^{-1}, with the gray scale indicated at the top. *Upper and lower insets:* Velocity profiles at the upper and lower points (marked with crosses), respectively. The systemic velocity is indicated with a caret, with increasingly positive velocities to the right.

IRWIN & SOFUE (see 396, L76)

no appreciable radial velocities at large *or* small radii, it appears that *rotating or collapsing ring models* can be ruled out. Although *molecular bars* which are offset from stellar bars (e.g., Kenney, Scoville, & Wilson 1991; Devereux, Kenney, & Young 1992), as well as molecular bars in the apparent absence of stellar bars (e.g., Sofue 1991), have now been observed in other galaxies, interpreting the tilted component as a molecular bar would require that it be physically inclined out of the plane of the galaxy, which seems unlikely.

The alternative is that *the tilted component is a consequence of the nuclear activity itself:* either a slowly ($\lesssim 30$ km s^{-1}) expanding ring or a collimated feature. Figure 4 shows a position/velocity plot along the *tilted component*. The dominant emission is from the main disk, with the tilted component visible as vertical, multicomponent, open-ended spurs centered on V_{sys} and extending out beyond the northwest and southeast boundaries of the main disk. This does not appear to be the signature of an expanding ring, which would show up as an elliptical feature with double-valued velocities at smaller radii and a single velocity at the largest radius. The almost constant velocity near V_{sys} at all radii, the open-endedness of the emission, and its presence at radii farther out than the main disk suggest that the tilted component is a collimated feature which may have a larger, unobserved component of velocity in the plane of the sky, i.e., the molecular gas is being accelerated outward by the nuclear jet.

Several other arguments support this view. The existence of the perpendicular spurs in a direction toward the radio lobes (Figs. 1 and 3) shows that the nuclear outflow is capable of accelerating at least some molecular clouds without destroying them. Indeed, the tilted component itself just resembles a spur to the northwest in the total intensity image (Fig. 1). Second, the tilted component, at P.A. $= -55°$, is *aligned* with the direction of the VLBI components (P.A. $= -57°$; Irwin & Seaquist 1988), i.e., it is aligned with the presumed "current" direction of outflow. And, third, there appears to be a weak extension at $r > 10''$ northwest, which is visible on the first (0.05 Jy beam^{-1}) contour of Figure 3 (see also the more obvious illustration in Fig. 4, frame 38, of Sofue & Irwin 1992), as if some of the molecular gas is continuing to move outward, beyond what should be the "edge" of the nuclear disk. The trailing curvature at large radii is associated with a velocity gradient in the same sense as normal galactic rotation and may be related to the turnover in the rotation curve. If this interpretation is correct, the kinetic energy of the outflow must be at least 10^{54} ergs, based on the minimum mass noted above and the 30 km s^{-1} radial velocity, and could be considerably higher if the outflow velocity is much greater than the observed radial velocity.

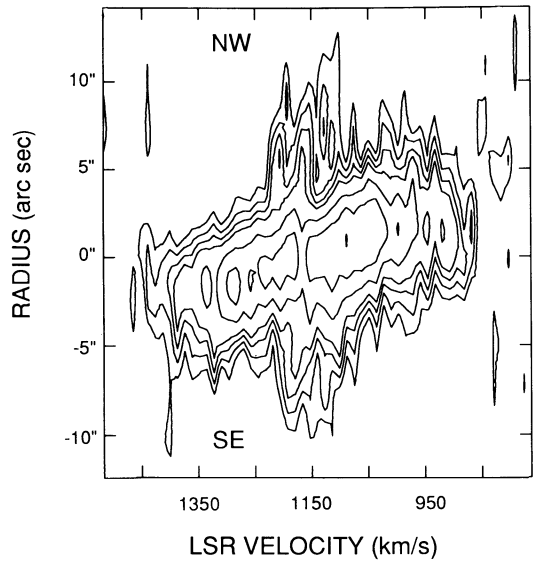

FIG. 4.—Position-velocity plot along the tilted component (P.A. $= -55°$), with the radius measured from the galaxy's center. Contours are at 0.15, 0.25, 0.35, 0.45, 0.70, 1.00, and 1.40 Jy beam^{-1}.

This situation appears to be very similar to that observed in NGC 4258, in which "anomalous arms" (i.e., nuclear jets) are also seen to curve in a trailing sense, and in which the molecular clouds have been interpreted by Plante et al. (1991) as "recoiling" due to the impact of the jet. Using pressure confinement arguments for the VLBI components (see Irwin & Seaquist 1988), we find that a jet, advancing into material of density 530 cm^{-3}, will have a velocity of *at least* 10^4 km s^{-1}. Following Plante et al. and using the minimum momentum flow of the jet (i.e., 4.5×10^{31} g cm s^{-2}, adjusted for distance; Irwin & Seaquist 1988), we find a jet power of $P_j > 4 \times 10^{40}$ ergs s^{-1}. This can be compared with *estimates* of 10^{43} ergs s^{-1} for NGC 4258 (Plante et al.), 3×10^{41}–3×10^{42} ergs s^{-1} for NGC 1068, and 5×10^{40}–5×10^{41} ergs s^{-1} for NGC 4151 (Wilson & Ulvestad 1982). Over a 10^6 yr period, therefore, the available kinetic energy from the jet would be greater than 10^{54} ergs, which, at least by order-of-magnitude estimates, is sufficient to power the CO outflow noted above.

5. RELATIONSHIP WITH THE RADIO CONTINUUM FEATURES

Figure 3 outlines the direction of the VLBI jet (*solid central bar*) as well as the identifiable radio continuum ridges and the boundaries of the radio lobes (*dashed curves*), as traced from the high-resolution (1.″4) image of Duric & Seaquist (1986, their Fig. 1*a*). In the northwest and southeast directions, the dashed curves are suggestive of an origin at the same angle as the VLBI jet and tilted CO component, with the outflow curving away from the galaxy's plane toward the minor axis. Exactly perpendicular to the VLBI angle are two additional brighter radio ridges toward the northeast and southwest. Two CO spurs are offset from these perpendicular ridges in Figure 3, but in matching resolution images they align quite well (see Sofue & Irwin 1992, Fig. 8*b*). The outflow from this galaxy has previously been interpreted as a high-velocity wide-angle bipolar wind (Duric & Seaquist 1988) or edge-brightened cone (Heckman, Armus, & Miley 1990; Filippenko & Sargent 1992). Although these data do not preclude the existence of such winds, the alignments illustrated here are suggestive of two distinct outflow directions—one at P.A. $= -56°$ northwest/southeast (VLBI jet direction, CO tilted component, and inner radio continuum ridge), and one perpendicular to this at P.A. $= +34°$ northeast/southwest (brightest radio continuum ridges and CO spurs)—with features farther from the nucleus and/or galactic plane aligning more closely with the galaxy's minor axis. These alignments could be consistent with biconical outflow if a single bipolar jet is precessing (e.g., Fujimoto & Sofue 1990) over a 90° angle (in projection). Since the two observed angles appear rather distinct, episodic outflow may be required in addition. An alternative suggestion is that a double or quadrupolar jet may be present. The latter possi-

bility is reminiscent of the spiral galaxy NGC 1097 (Wehrle, Keel, & Jones 1991 and references therein), in which two bipolar optical jets extend from the nucleus. Perhaps NGC 1097 represents a later, more quiescent phase when gaseous outflow from the nucleus has ceased.

This work was financially supported by the Ministry of Education, Science and Culture under grants 01420001 and 01302009 (Y. S.), and the National Research Council of Canada and Natural Sciences and Engineering Research Council of Canada (J. I.).

REFERENCES

Bania, T. M. 1977, ApJ, 216, 381
Devereux, N. A., Kenney, J. D. P., & Young, J. S. 1992, AJ, 103, 784
Duric, N., & Seaquist, E. R. 1986, Canadian J. Phys., 64, 531
———. 1988, ApJ, 326, 574
Duric, N., Seaquist, E. R., & Davis, L. E. 1983, ApJ, 273, L11
Filippenko, A. V., & Sargent, W. L. W. 1992, AJ, 103, 28
Ford, H. C., Dahari, O., Jacoby, G. H., Crane, P. C., & Ciardullo, R. 1986, ApJ, 293, 132
Fujimoto, A. D., & Sofue, Y. 1990, in IAU Symp. 140, Galactic and Intergalactic Magnetic Fields, ed. R. Beck, P. P. Kronberg, & R. Wielebinski (Dordrecht: Kluwer), 377
Haschick, A. D., & Baan, W. A. 1985, Nature, 314, 144
Heckman, T. M., Armus, L., & Miley, G. K. 1990, ApJS, 74, 833
Hummel, E., van Gorkom, J. H., & Kotanyi, C. G. 1983, ApJ, 267, L5
Irwin, J. A., & Seaquist, E. R. 1988, ApJ, 335, 658
———. 1990, ApJ, 353, 469
———. 1991, ApJ, 371, 111
Kenney, J. D. P., Scoville, N. Z., & Wilson, C. D. 1991, ApJ, 366, 432
Plante, R. L., Lo, K. Y., Roy, J.-R., Martin, P., & Noreau, L. 1991, ApJ, 381, 110
Scoville, N. Z., & Sanders, D. B. 1987, in Interstellar Processes, ed. D. J. Hollenbach & H. A. Thronson, Jr. (Dordrecht: Reidel), 21
Sofue, Y. 1988, in Molecular Clouds in the Milky Way and External Galaxies, ed. R. L. Dickman, R. L. Snell, & J. S. Young (Berlin: Springer-Verlag), 375
———. 1991, in IAU Symp. 146, Dynamics of Galaxies and Their Molecular Cloud Distributions, ed. F. Combes & F. Casoli (Dordrecht: Kluwer), 287
Sofue, Y., & Irwin, J. 1992, PASJ, in press
van Gorkom, J. H., & Ekers, R. D. 1986, in Synthesis Imaging, ed. R. A. Perley, F. R. Schwab, & A. H. Bridle (NRAO), 177
Wehrle, A. E., Keel, W. C., & Jones, D. L. 1991, in ASP Conf., Vol 18, The Interpretation of Modern Synthesis Observations of Spiral Galaxies, ed. N. Duric & P. C. Crane (San Francisco: ASP), 251
Wilson, A. S., & Ulvestad, J. S. 1982, ApJ, 263, 576
Young, J. S., Claussen, M. J., & Scoville, N. Z. 1988, ApJ, 324, 115
Young, J. S., & Scoville, N. Z. 1982, ApJ, 258, 467
———. 1991, ARA&A, 29, 581

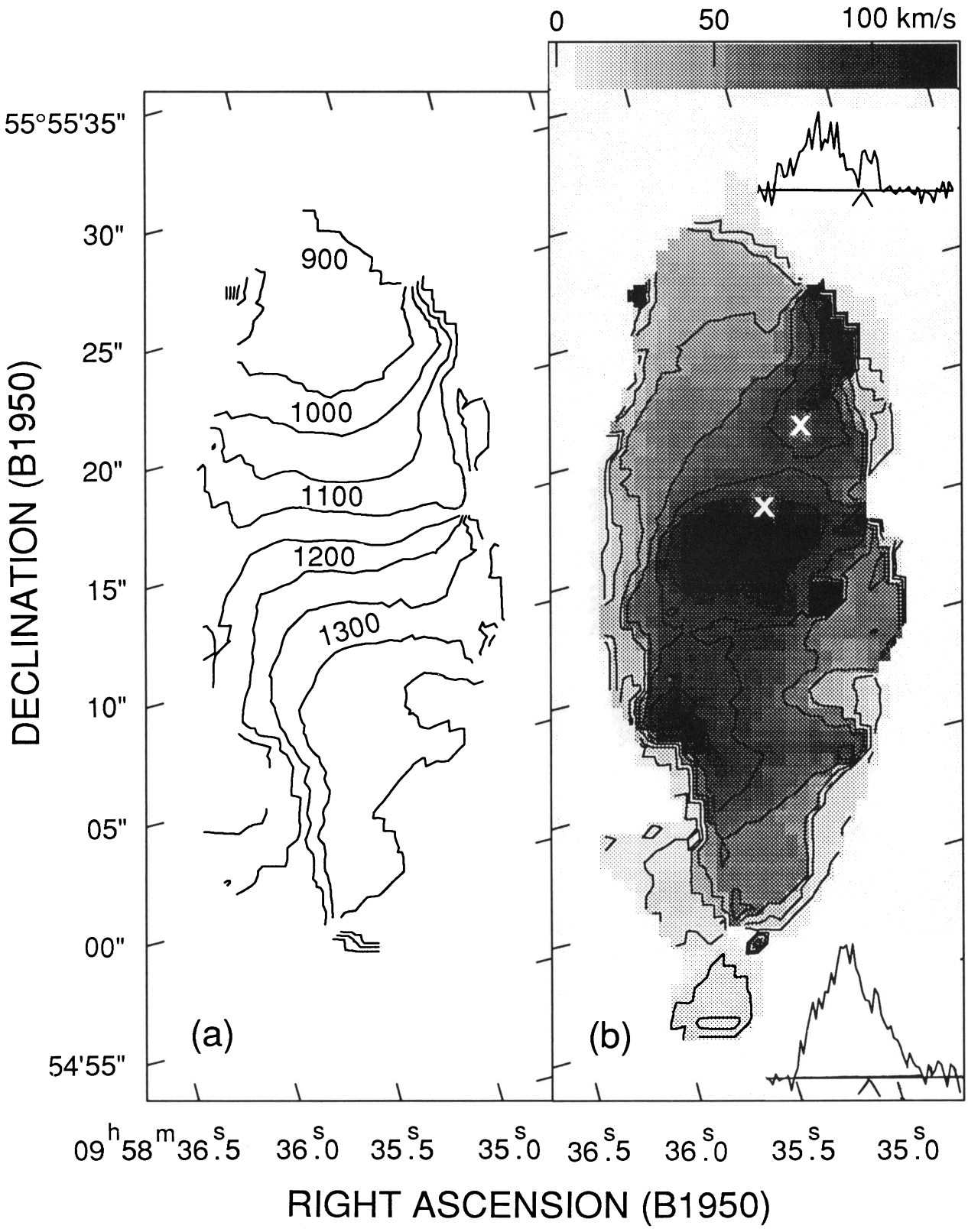

FIG. 2.—(*a*) Mean velocity field of NGC 3079, with the major axis vertical. Contours are separated by 50 km s^{-1}, with LSR velocities indicated on every other contour. (*b*) Velocity dispersion. Contours are 10, 25, 50, 75, 95, and 110 km s^{-1}, with the gray scale indicated at the top. *Upper and lower insets:* Velocity profiles at the upper and lower points (marked with crosses), respectively. The systemic velocity is indicated with a caret, with increasingly positive velocities to the right.

IRWIN & SOFUE (see 396, L76)